Finite Orbit Monte-Carlo Simulation of Ion Cyclotron Resonant Heating Scenarios in DIII-D, NSTX, KSTAR and ITER

M. Choi 1), D.L. Green 2), E.F. Jaeger 3), V.S. Chan 1), C.M. Muscatello 4), W.W. Heidbrink 4), D. Liu 5), R.W. Harvey 6), L.L. Lao 1), R.I. Pinsker 1), L.A. Berry 2), P. Bonoli 7), S.H. Kim 8) and RF-SciDAC Team

1) General Atomics, P.O. Box 85608, San Diego, California 92186-5608, USA
2) Oak Ridge National Laboratory, P.O. Box 2008, Oak Ridge, Tennessee 37831-6169, USA
3) XCEL Engineering Inc., 1066 Commerce Park Dr., Oak Ridge, Tennessee 37830, USA
4) University of California-Irvine, Irvine, California 92697, USA
5) University of Wisconsin-Madison, Wisconsin, 53706, USA
6) CompX, P.O. Box 2672, Del Mar, California 92014-5672, USA
7) Massachusetts Institute of Technology, Cambridge, Massachusetts 02139, USA
8) KAERI, Daeduk-Daero 1045, Dukjin-dong, Yuseong-gu, Daejeon, 305-353, Korea

e-mail contact of main author: choi@fusion.gat.com

Abstract. Iterative simulations of 5-D finite-orbit Monte-Carlo code ORBIT-RF coupled with 2-D full-wave code All-ORders Spectral Algorithm AORSA including quasi-linear and collisional orbit diffusion reproduce qualitatively experimental observations in enhanced neutron reaction rates and outward spatial shifts of fast ions from the magnetic axis in DIII-D and NSTX moderate to high harmonic ICRF heating experiments. The outward shift of fast ions comes from large orbit drifts of fast ions across the magnetic surfaces, which cannot be reproduced when finite drift orbit effect is ignored. Preliminary ORBIT-RF/AORSA simulations for proposed fundamental minority ICRF heating scenarios in ITER and KSTAR show flat or asymmetric minority fast ion distributions, which are different from those predicted from conventional zero-orbit simulations. The results suggest that finite drift orbit effect of fast ions may also be important in modeling ICRF minority heating experiments in these devices.

1. Introduction

Waves in the ion cyclotron range of frequency (ICRF) are one of the main auxiliary plasma heating and current drive methods in DIII-D [1], NSTX [2], KSTAR [3] and ITER [4]. On DIII-D and NSTX, ICRF waves with frequencies equivalent of moderate to high ion cyclotron harmonic number (3rd to 12th) have been launched into neutral beam (NB) preheated plasma to heat electrons and drive plasma current non-inductively. However, partial or strong damping of ICRF waves by NB fast ions with enhanced neutron emission rate has been observed [5–7]. Theory predicts that this parasitic absorption of ICRF waves by NB fast ions may occur due to finite Larmor radius (FLR) effect where $k_\perp \rho_i \geq 1$ ($k_\perp$ is the perpendicular wave number and ρ_i is the fast ion Larmor radius) [8]. The spatial profile of NB fast ion density measured by fast ion D_α (FIDA) [9] spectroscopy during ICRF heating indicated that the peaks move outwards from the primary resonance layers located near the magnetic axis [6,7]. Theory suggests that this shift can be due to finite drift orbit width effect of fast ions across the magnetic flux surfaces [8], which can modify local fast ion distribution function and consequently may affect the ICRF wave propagation and absorption in the plasma.

To improve the theoretical understanding of resonant interactions of fast ions with ICRF waves including finite drift orbit and FLR effects, we investigate the self-consistent interaction of NB fast ions with ICRF waves using the 5-D finite-orbit Monte-Carlo code ORBIT-RF [10] coupled with the 2-D full wave code AORSA [11,12]. Preliminary results from a previous study qualitatively reproduced experimental observations in both enhanced neutron reaction rates and outward shifts of fast ion density from the magnetic axis in

moderate harmonic DIII-D and high harmonic NSTX ICRF heating experiments [13]. They also showed that finite drift orbit effect of fast ions and iterative simulation between fast ion distribution and ICRF wave absorption/propagation are important in modeling ICRF heating experiments [13]. A main discrepancy was that ORBIT-RF/AORSA computed stronger outward shifts than those indicated by the FIDA signals. In these comparisons, to get reliable count statistics, the FIDA fast ion density data is averaged over a fairly long time window (500 ms) in the DIII-D discharge [6], whereas in the NSTX discharge it is averaged over 70 ms [7]. To investigate the effects due to data average on the discrepancy, we have extended the simulations over similar experimental time windows as well as extracted fast ion data over 20 timeslices to improve statistics.

Proposed ICRF heating scenarios in KSTAR include fundamental minority hydrogen (H) heating in deuterium (D) plasma at full magnetic field (3.0 T) or second harmonic at half field with 3 to 6 MW of ICRF power. In ITER, 20 MW of ICRF power is planned to heat the plasma with minority helium-3 (He^3) or D in tritium (T) plasma. In addition, a large population of fusion-born 3.5 MeV alpha particles exists simultaneously. The existence of fast ions in the form of minority species heated by ICRF hearting process or alpha particles in KSTAR and ITER may significantly modify the fast ion distribution due to their large drift orbit motion and associated loss of fast ions to the wall. To investigate the finite orbit effects on the minority fast ion distribution, we have concentrated on the fundamental harmonic minority heating scenarios in ITER and KSTAR at the high ICRF power. Preliminary results from ORBIT-RF/AORSA indicate that finite drift orbit effects may also be important in these devices.

In this paper, first we present latest comparison results of ORBIT-RF coupled with AORSA against FIDA signals in DIII-D and NSTX ICRF heating experiments. Then we present preliminary modeling results from ORBIT-RF/AORSA for the fundamental harmonic minority heating scenarios in ITER and KSTAR and comparison with simulation results assuming zero-orbit width.

2. Fast ion distribution in NB heating experiments

In this section, we compute NB fast ion distribution with ORBIT-RF using NB heating experimental parameters without ICRF heating and validate ORBIT-RF simulation results against FIDA signals. This validation work is important for quantitative understanding of resonant interactions of NB fast ions with ICRF waves in NB + ICRF heating experiments in NSTX and DIII-D discussed in the next section.

In ORBIT-RF simulations, only the full energy component of the injected NB source is considered. Since fast ion contribution from half and one-third energy components to FIDA are ignorable due to very little acceleration of low energy ions [6], modeling of NB fast ions with a single full energy component is not expected to affect significantly the comparison of ORBIT-RF results against FIDA. The presence of MHD activities such as sawteeth or compressional Alfvén eigenmodes (CAE) in the plasma can lead to non-classical fast ion distribution. However, the effect of MHD on the fast ion distribution is ignored in these simulations. In these first comparisons, only normalized spatial profiles of fast ion computed by ORBIT-RF are compared with those from FIDA. More detailed comparison using un-normalized fast ion data is underway.

In these simulations, ORBIT-RF is typically run for a few slowing down times including the collisional orbit diffusion effects. To improve statistics associated with extracting fast ion information from ORBIT-RF, we have enhanced ORBIT-RF to record instantaneous fast ion data 20 times over the last 60 ms of simulation time (from 200 to 260 ms). The results are shown in Fig. 1, where the spatial profile of FIDA signals computed by the synthetic

diagnostic code "FIDASIM" [14] using fast ion distribution from ORBIT-RF (red lines) is compared against those from FIDA measurements (symbols with error bars) for a NSTX discharge before application of ICRF waves (#128742). In this discharge, the D beam injection energy is 65 keV, NB power is 1 MW, tangency radius is 0.59 m, the central electron density is $n_e(0) \approx 3.3 \times 10^{13}\,\mathrm{cm}^{-3}$, the central electron temperature is $T_e(0) \approx 1.4$ keV and the central ion temperature is $T_i(0) \approx 1.0$ keV. The dotted vertical line indicates the magnetic axis. As shown in Fig. 1, good agreement is obtained in normalized spatial profile of FIDA signals against ORBIT-RF results.

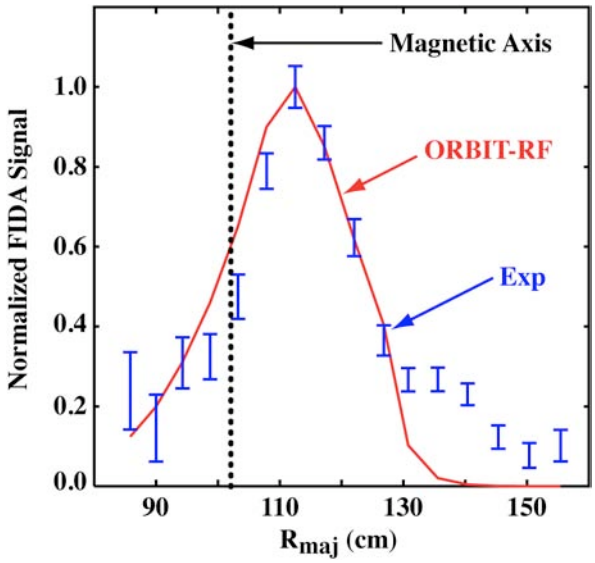

FIG. 1. Comparison of normalized spatial profile of FIDA signals computed by the synthetic diagnostic code FIDASIM using ORBIT-RF fast-ion distributions (red lines) against FIDA measurements (symbols with error bars) for the NSTX discharge #128742 before ICRF heating.

3. Resonant interactions of NB or minority fast ions with ICRF waves

3.1. NB + high harmonic ICRF heating: NSTX #128739

In NSTX ICRF discharge (#128739), 1.0 MW of 65 keV deuterium neutral beam is injected into the plasma from 150 to 400 ms in the direction of the plasma current (0.8 MA) at a tangency radius of 0.59 m. The major radius at the magnetic axis is $R_0 = 1.04$ m, the minor radius is $a = 0.67$ m, and the toroidal magnetic field at the magnetic axis is $B_0 = 0.55$ T. From 210 to 370 ms, 1.0 MW of ICRF power is launched into the plasma with a twelve-strap antenna. The applied ICRF wave frequency is 30 MHz with a peak in the vacuum spectrum $k_{||} = 7\ \mathrm{m}^{-1}$. At this B_0, the 30 MHz ICRF wave interacts with D ions at several ion cyclotron resonance layers (3rd to 11th) that are closely located along the major radius, as shown in Fig. 2. The 8th layer is located near the magnetic axis. The plasma parameters are $n_e(0) \approx 3.2 \times 10^{13}\,\mathrm{cm}^{-3}$, $T_e(0) \approx 1.4$ keV and $T_i(0) \approx 1.0$ keV. Measured D-D neutron emission (mostly from D beam-D plasma reactions) increases continuously up to about a factor of three during the ICRF heating phase [7].

For this comparison, ORBIT-RF/AORSA is run for 150 ms including quasi-linear and collisional orbit diffusion using ORBIT-RF computed NB fast ion distribution as an initial condition. Fast-ion distribution and ICRF wave fields are updated every 50 ms. The results are shown in Fig. 2, where the computed spatial profile of FIDA signals after application of

the ICRF waves are compared against the FIDA signals measured from the tangential viewing chords. For this comparison, FIDA signals with ICRF is normalized by that without ICRF. Good agreement is obtained, although the simulation computes a slightly enhanced outward shift than that from measurement. ORBIT-RF/AORSA indicates that about 30% of ICRF power is absorbed by NB fast ions.

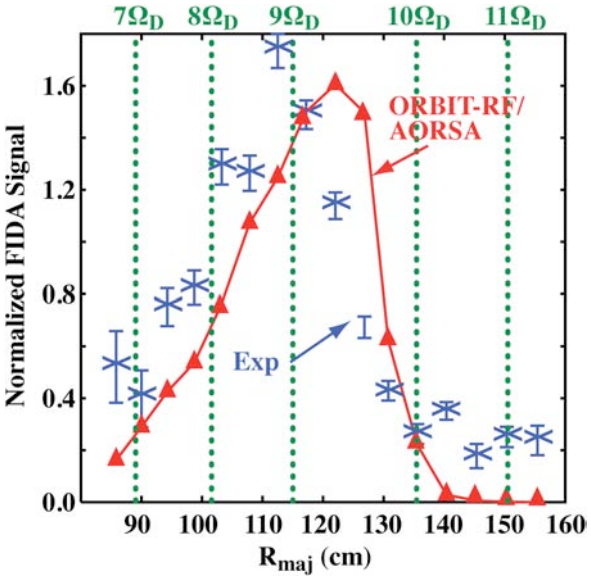

FIG. 2. Comparison of spatial profile of FIDA signals computed by the synthetic diagnostic code FIDASIM using ORBIT-RF fast-ion distributions (red line with Δ) against FIDA signals (X with error bars) for NSTX ICRF heating discharge #128739.

3.2. NB + moderate harmonic ICRF heating: DIII-D #122993

In DIII-D ICRF discharge (#122993), neutral beam injects 1.2 MW of 80 keV D ions into the plasma from 1200 to 4000 ms in the direction of the plasma current (1.0 MA) at a tangency radius of 1.15 m. R_0=1.75 m, a=0.6 m and B_0=1.54 T. After neutral beam preheats the plasma, 1.0 MW of ICRF power is coupled to the plasma for a 1500 ms pulse (from 2000 to 3500 ms). Four-element phased array is used to launch the 60 MHz ICRF wave into the plasma at $k_{\|} = 5$ m^{-1}. At this B_0, the 60 MHz ICRF wave interacts with D ions at three cyclotron resonance layers along the major radius, the 4th harmonic at $R = 1.36$ m, the 5th at $R = 1.74$ m, and the 6th at $R = 2.06$ m. As shown in Fig. 3, the resonant layers are well separated and resonant interaction occurs mostly at the 5th harmonic near the magnetic axis. The plasma parameters are $n_e(0) = 3.3 \times 10^{13}$ cm^{-3}, $T_e(0) = 2.0$ keV and $T_i(0) = 2.1$ keV. Measured D-D neutron emission rate increases about a factor of two during the first 200 ms and then becomes stationary [6].

In this DIII-D comparison, the FIDA signals are averaged over 500 ms to get reliable count statistics [6]. ORBIT-RF is run for 560 ms with the ICRF wave fields computed from AORSA. Both fast ion distribution and ICRF wave fields are updated every 70 ms. The computed enhanced neutron rate is 2.2, which is in good agreement with the measured value of 2.4. The results are shown in Fig. 3, where the spatial profile of FIDA signals measured from the vertical viewing chords during the ICRF heating phase are compared against ORBIT-RF/AORSA results. Again FIDA signals with ICRF is normalized by that without ICRF. As shown in Fig. 3, ORBIT-RF/AORSA simulations produce qualitatively off-axis radial profile similar to that from the FIDA measurement. However, in the central region,

FIDA measurements indicate a much larger enhancement factor than that from ORBIT-RF/AORSA, although the uncertainty in this experimental measurement is large. As indicated in the previous study [13], comparison with zero-orbit simulations suggests that this radial shift is due to finite orbit width effects of fast ions across the magnetic surfaces. ORBIT-RF/AORSA indicates that about 70% of ICRF power is absorbed by NB fast ions.

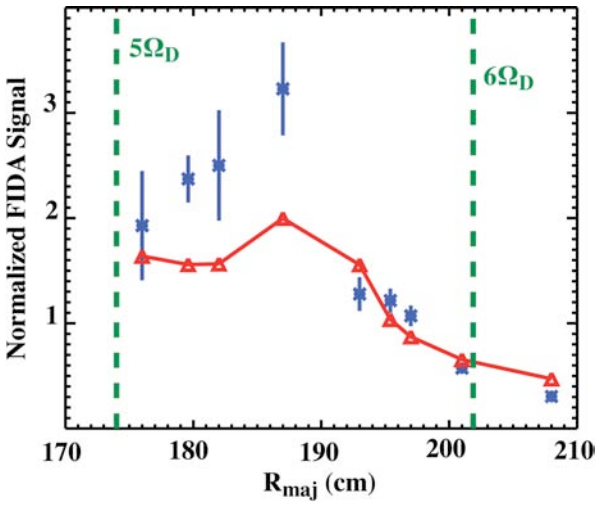

FIG. 3. Comparison of spatial profile of FIDA signals computed by the synthetic diagnostic code FIDASIM using ORBIT-RF fast-ion distributions (red line with Δ) against FIDA measurements (X with error bars) for DIII-D ICRF heating discharge #122993.

3.3. Fundamental harmonic ICRF heating: ITER

To understand the quasi-linear interaction of minority fast ions with ICRF waves at high power in ITER, the proposed fundamental harmonic heating scenario of D minority ions in majority tritium (T) plasma at full field B_0 = 5.3 T is simulated using the magnetic geometry of ICRF heating scenario 4 [11]. The concentration of minority ions is assumed to be 10%. Plasma parameters are $n_e(0) \approx 7.3 \times 10^{13}$ cm^{-3}, $T_e(0) \approx$ 24 keV and $T_T(0) \approx 25$ keV. The ICRF wave frequency is set to be 40 MHz to position the D fundamental resonance near the magnetic axis. The ICRF power is P_{RF} = 20 MW. Minority ions are assumed initially to have a Maxwellian distribution, as shown in Fig. 4(a). Existence of possible fusion alpha species is ignored in this simulation. A single toroidal mode number n_φ = –35 is used. ORBIT-RF is run for 120 ms with fast ion distribution and ICRF waves updated every 30 ms.

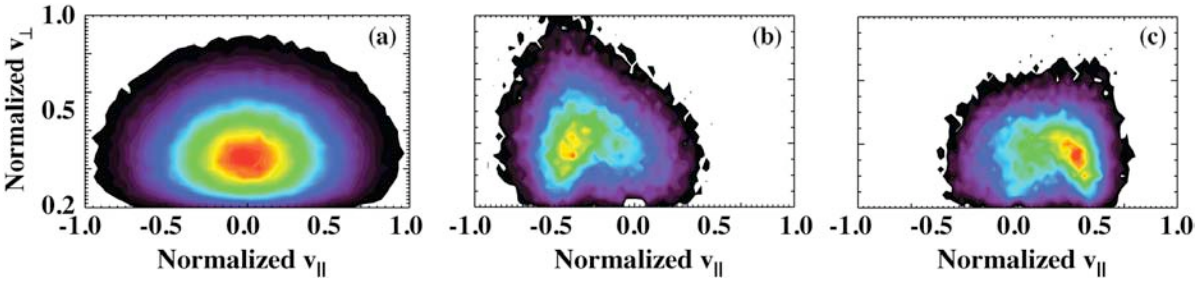

FIG. 4. Contour plots of ICRF heated D minority ion particle distribution computed by ORBIT-RF/AORSA at (a) $t = 0$, (b) at t = 120 ms near ρ = 0.1 and (c) at t = 120 ms near ρ = 0.4 for an ITER ICRF scenario.

In Fig. 4(b) and (c), contour plots of ICRF heated minority ion particle distributions in velocity space are shown near ρ = 0.1 [Fig. 4(b)] and ρ = 0.4 [Fig. 4(c)] at t = 120 ms. For comparison, the results predicted from AORSA/CQL3D [15] assuming zero-orbit are shown at similar radii in Fig. 5. As shown in Figs. 4(b) and 5(a), near the magnetic axis

ORBIT-RF/AORSA and AORSA/CQL3D show similar asymmetric rabbit ear distributions toward the left side (negative n_φ). However, ORBIT-RF/AORSA produces relatively flat distribution near $\rho = 0.4$ [Fig. 4(c)] while as AORSA/CQL3D computes typical symmetric rabbit ear distribution [Fig. 5(b)]. This difference may be due to finite drift orbit width effect of minority tails in this particular ICRF heating scenario. To assess finite orbit effect on this difference, we run ORBIT-RF/AORSA by turning the drift orbit terms off. The result is shown in Fig. 6. As expected, without the drift terms ORBIT-RF/AORSA also computes typical symmetric rabbit ear distribution consistent with AORSA/CQL3D [Fig. 5(b)].

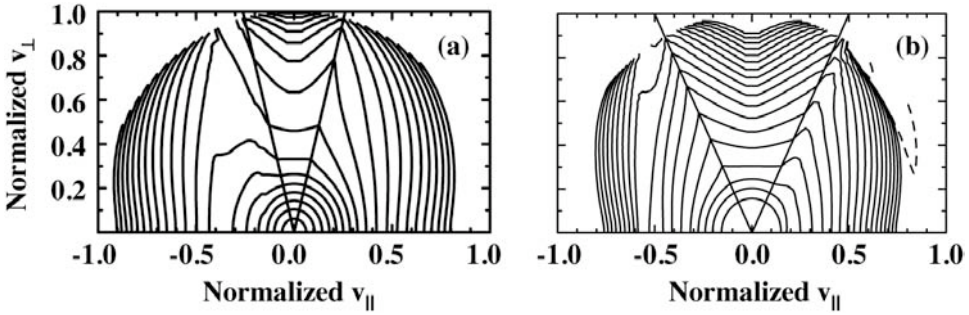

FIG. 5. Contour plots of ICRF heated D minority ion distribution computed by AORSA/CQL3D at (a) $\rho = 0.1$ and (b) $\rho = 0.4$ for an ITER ICRF scenario.

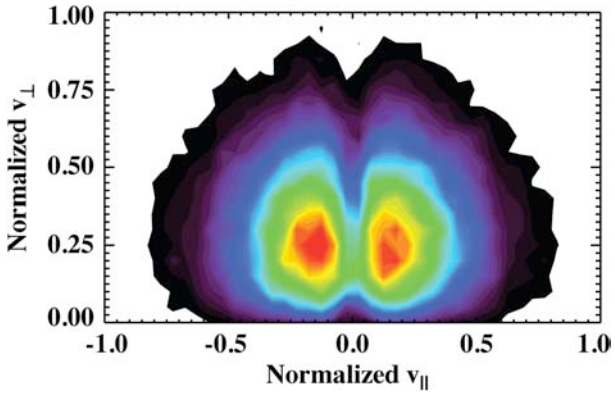

FIG. 6. Contour plot of ICRF heated D minority ion particle distribution computed by ORBIT-RF/AORSA near $\rho = 0.4$ for an ITER ICRF scenario when drift orbit terms are ignored.

3.4. Fundamental harmonic ICRF heating: KSTAR

Preliminary simulations have also been performed for a proposed ICRF heating scenario in KSTAR, fundamental H minority heating in D plasma at full magnetic field $B_0 = 3.0$ T with 6 MW of ICRF power. Concentration of minority ions is assumed to be 10%. Plasma parameters are $n_e(0) \approx 6.7 \times 10^{13}$ cm^{-3}, $T_e(0) \approx 2$ keV and $T_D(0) \approx 2$ keV. H minority ions are assumed to have a Maxwellian distribution initially. The ICRF wave frequency is set at 45 MHz and toroidal mode number is $n_\varphi = 19$. ORBIT-RF is run only for ~ 10 ms (~a half of slowing down time) with the fast ion distribution and ICRF waves updated every 2 ms. The results are given in Fig. 7, where a contour plot of the ICRF heated minority H particle distribution at t=10 ms near $\rho = 0.4$ is shown. The fast ions show a strongly asymmetric rabbit ear distribution toward the right hand side (positive n_φ). As discussed in the previous section, this asymmetry comes from the drift orbit effects of the minority tails in this

particular ICRF heating scenario. Simulations without the drift orbit terms produces symmetric rabbit ear distribution, as expected.

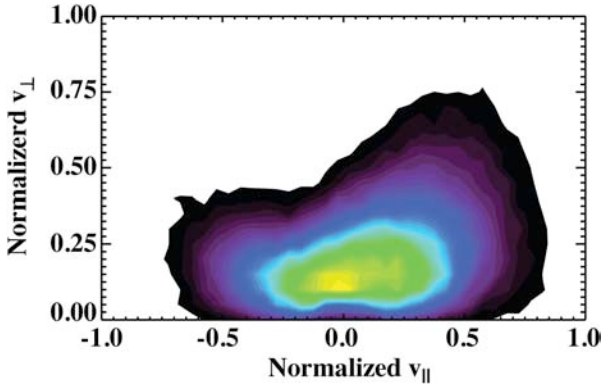

FIG. 7. Contour plot of ICRF heated H minority ion particle distribution computed by ORBIT-RF/AORSA near ρ=0.4 for a KSTAR ICRF scenario.

4. Summary

Iterative simulations of ORBIT-RF/AORSA with quasi-linear and collisional orbit diffusion reproduce qualitatively experimental observations in enhanced neutron reaction rates and outward shifts of fast ions from the magnetic axis in both moderate harmonic DIII-D and high harmonic NSTX ICRF heating experiments. The outward radial shift of fast ions comes from large orbit drifts across the magnetic surfaces, which cannot be reproduced when the finite drift orbit effect is ignored. A noted discrepancy is that ORBIT-RF/AORSA computes slightly stronger outward shift than the FIDA signals in the NSTX case and less fast-ion enhancement near the plasma center region in the DIII-D case.

This discrepancy may be due to several missing physics elements in the ORBIT-RF model. First, parallel acceleration is not included in this work that may affect pitch-angle and energy distribution. As a result, the fast ion radial excursion may be affected. Secondly, the perpendicular wavenumber and the phase difference between $E+$ and $E-$, which are required in computing the Bessel function that accounts for the FLR effects, are computed using the cold plasma dispersion relation in ORBIT-RF. Thirdly, the incoming ICRF wave fields are represented using only one peak n_φ. Lastly, the up-shift in $k_{||}$ due to the poloidal magnetic field is also not included.

Preliminary ORBIT-RF/AORSA simulations for the proposed ICRF heating scenarios in ITER and KSTAR show flat or strongly asymmetric minority fast ion distributions, which are different from those predicted from conventional zero-orbit simulations that show symmetric rabbit ear structures. The results suggest that finite drift orbit effect of minority fast ions may also be important in modeling ICRF minority heating in these devices.

Acknowledgment

This work was supported in part by the US Department of Energy under DE-FG02-95ER54309, DE-FC02-04ER54698, DE-AC05-00OR22725, SC-G903402, DE-FG02-92ER54139, DE-FG02-99ER54541, DE-FG02-94ER54235 and DE-FC02-08ER54952.

References

[1] LUXON, J.L., Nucl. Fusion **42**, 614 (2002).
[2] ONO, M., *et al*., Nucl. Fusion **41**, 1435 (2001).
[3] LEE, G.S., *et al*., Nucl. Fusion **40**, 575 (2000).
[4] AYMAR, R., *et al*., Nucl. Fusion **41**, 1301 (2001).
[5] PINSKER, R.I., *et al*., Nucl. Fusion **46**, S416 (2006).
[6] HEIDBRINK, W.W., *et al*., Plasma Phys. Control. Fusion **49**, 1457 (2007).
[7] LIU. D, *et al*., Plasma Phys. Control. Fusion **52** (2010).
[8] HEDIN. J, *et al*., Theory of Fusion Plasma (Proc. Joint Varenna-Lausanne Workshop Varenna, 1998) Editrice Compositori (1999) p. 467, ISBN88-7794-167.
[9] HEIDBRINK, W.W., *et al*., Plasma Phys. Control. Fusion **46**, 1855 (2004).
[10] CHOI, M., *et al*., Phys. Plasmas **16**, 052513 (2009).
[11] JAEGER, E.F., *et al*., Phys. Plasmas **9**, 1873 (2002).
[12] GREEN, D.L., *et al*., AIP Conf. Proc. **1187**, 569 (2009).
[13] CHOI, M., *et al*., Phys. Plasmas **17**, 056102 (2010).
[14] HEIDBRINK, W.W., et al., "A code that simulates fast-ion D-alpha and neutral particle measurements," Comm. Comp. Physics **8** (2010) submitted.
[15] HARVEY, R.W., *et al*., USDOC NTIS document DE93002962.7, 4609 (2000).